

XPS, EM, and Catalytic Studies of the Accumulation of Carbon on Pt Black

N. M. Rodriguez,* P. E. Anderson,* A. Wootsch,† U. Wild,‡ R. Schlögl,‡ and Z. Paál†,‡,1

*Department of Chemistry, Northeastern University, Boston, Massachusetts 02115; †Chemical Research Center, Institute of Isotope and Surface Chemistry, Hungarian Academy of Sciences, P.O. Box 77, Budapest H-1525, Hungary; and ‡Fritz-Haber-Institut der MPG, Faradayweg 4-6, D-14195 Berlin, Germany

Received August 7, 2000; revised September 25, 2000; accepted September 28, 2000; published online December 21, 2000

Pt black samples were exposed to 2,4-hexadiene (24HD) at 603 and 693 K, alone or in the presence of excess hydrogen. The 24HD underwent C=C double-bond shift, geometric isomerization, and minor aromatization during its contact with Pt in the absence of H₂. It was hydrogenated to hexenes and hexane when hydrogen was present. Test runs with an *n*-hexane–hydrogen mixture after 24HD treatment showed a more pronounced decrease of activity and a loss of isomerization/cyclization selectivities after exposure without hydrogen. The amount, structure, and possible chemical state of residual carbon were examined by transmission electron microscopy (TEM) and X-ray photoelectron spectroscopy (XPS). The sintered metal contained some inherent (likely harmless) carbon impurity, the amount of which increased upon exposure to 24HD to 44–50%, higher temperatures and lower H₂ concentration resulting in more solid carbon. Regeneration by an O₂–H₂ treatment removed much, but not all, of the solid carbon deposit. Difference spectra of hexadiene-treated and regenerated samples showed an excess of graphite in the carbonized samples whereas Pt/C was more abundant after regeneration, in agreement with C 1s line fitting. Transmission electron microscopic examinations showed mainly pyrolytic carbon. Graphitic layers (not highly ordered ones) perpendicular to the Pt surface were identified after exposure to 24HD/H₂ mixtures of various composition. Graphitic and amorphous C caused a nonselective deactivation. Difference C 1s spectra showed a component with a binding energy at ~284.1 between graphite and Pt/C. The suppression of the catalytic propensities in skeletal reactions (isomerization and C₅ cyclization) and the difficulty of self-reactivation in the prolonged test runs were consistent with the presence of this type of deposit representing, likely, a disordered nongraphitic hydrocarbon oligomer. © 2001 Academic Press

Key Words: Pt black, carbonization; graphite on Pt: identification by TEM; XPS and UPS of carbonized Pt; 2,4-hexadiene; *n*-hexane reactions on deactivated Pt.

INTRODUCTION

The presence of carbonaceous entities has been shown to be the normal state of Pt catalysts during skeletal rear-

rangement reactions of >C₆ hydrocarbons (aromatization, C₅ cyclization, isomerization, hydrogenolysis) taking place in the range of 570–770 K (1–3). Counterclaims have appeared concerning the form, amount, and chemical state of this carbon deposit. Webb (4) defined such materials as “hydrocarbonaceous deposits,” indicating that they are probably closer to dehydrogenated hydrocarbons in the chemisorbed state than to “coke.” Somorjai and co-workers (1, 2) distinguished three-dimensional (3D) carbonaceous polymers, individual C atoms attached to Pt atoms, and assumed that clean Pt islands were also present to perform the catalytic reactions. Sárkány (5, 6) used a hydrogen flushing step after reacting *n*-hexane on various Pt catalysts and found that this procedure could remove up to 2 C atoms per surface Pt (Pt_s). Garin *et al.* (7) pointed out that hydrogen flushing could remove most of the chemisorbed hydrocarbons from Pt single crystals that otherwise would form coke, observed several times after evacuating the system.

In spite of several studies (2, 4, 6, 7), the nature, amount, and chemical state of carbon accumulating during hydrocarbon reactions are still not certain. The amount of carbon present on Pt black was not negligible, even after customary regeneration with O₂ and H₂ (8, 9). This residual carbon contained mainly graphite and C_xH_y polymers together with some oxygenated C species (8). The coexistence of ordered and disordered C species agreed well with earlier reports (10). Since the regenerative treatments restored the activity of Pt in a well-reproducible way, we may assume that carbon existed partly in the form of 3D deposits (1, 8, 11) blocking a part of the surface and leaving a sufficient fraction free and available for catalytic reactions. At the same time, XPS revealed that regeneration enhanced the relative abundance of C/Pt entities, very likely as single C atoms or chemisorbed CH_x species (12, 13). The polymerization of these species may represent one possible route of coking (14). This pathway may involve dissolution of these C atoms into the metal preferred at higher temperature. Indeed, a hydrogen treatment of a rather clean Pt black surface increased its carbon content, likely due to the

¹ To whom correspondence should be addressed. Fax: (361) 392 2533. E-mail: paal@iserv.iki.kfki.hu.

reappearance of carbon atoms on the surface (15). These entities may serve as precursors of graphite formation (16). The chemistry of various forms of carbon and their interconversion has been treated in detail by one of the authors (17).

3D carbon islands block a fraction of the catalytic surface, thus causing the activity to drop. Single C atoms, in turn, may create Pt–C ensembles (18), affecting, first of all, selectivities (12). The gradual increasing of surface carbonization tended to initially interfere with isomerization, resulting in enhancement of the abundance of C₅ cyclics. A massive deactivation by carbon, in turn, prevented all skeletal rearrangement reactions, leaving the dehydrogenating activity more or less intact (19, 20). The activity drop was slower in excess H₂ (9, 20, 21). At the same time, the presence of H₂ slowed down both “useful” and “deactivating” reactions on Pt, leading eventually to the accumulation of larger amounts of surface carbon (22). Increasing hydrogen pressure, on the other hand, increased the augmented amount of solid carbon produced from both ethylene and acetylene, possibly due to the prevention of the growth of surface graphite and the concomitant promotion of the dissolution of C atoms in Pt (16). Such phenomena should be accompanied by a solid-state rearrangement of dispersed Pt particles, exhibiting a “flexible surface” (23). X-ray diffraction (13) confirmed that an anisotropic rearrangement can occur at temperatures as low as ~500 K, as opposed to the values of 700–1300 K reported earlier (10, 24, 25). It was suggested that hydrogen was required for this process (13, 26).

So far, methods of surface science, such as X-ray and ultraviolet photoelectron spectroscopy (XPS, UPS) (7, 8, 11), Auger electron spectroscopy (AES) (1, 3, 27), work function measurements (27), and secondary ion mass spectrometry (SIMS) (28), have been used to detect surface carbon on Pt. The formation of massive amounts of carbon on Pt black started at 650 K and increased up to ca. 900 K (16). The formation of a spirally stacked 3D graphite needle from gas-phase ethylene and cyclohexene at 633 K (29) was observed by electron microscopy. As far as we know, no other direct EM observation of carbonaceous overlayers on Pt has been reported.

The present paper includes a study of controlled carbonization of Pt catalyst upon exposure to a hydrocarbon, *trans,trans*-2,4-hexadiene (24HD), under various conditions. Exposures of different severity were carried out twice: in a catalytic reactor with product analysis and in the preparation chamber of the electron spectrometer. In the former case, the transformation of 24HD as well as the residual activity was checked. In the latter case, the amount and probable chemical state of C on Pt were monitored by XPS and UPS. Electron microscopic examinations were carried out with some of the latter samples in an attempt to establish if direct observation of surface carbon and its morphological characteristics was possible. The com-

bination of these methods will present direct experimental evidence on the structure and activity of the—partly carbonized—Pt surface. We used Pt black as the model catalyst (9, 15, 30), exposing different surface planes, thus being closer to real-world disperse catalysts but lacking support effects interfering possibly with XP and UP spectroscopy and eliminating support effects during carbon accumulation (14, 31).

METHODS

Catalyst

Pt black was prepared by reduction of an aqueous solution of H₂PtCl₆ by HCHO in the presence of concentrated KOH (9, 32). The K impurity was removed by washing the sample with diluted HNO₃. The original fine particles (sample **1**) were presintered to sample **2** in H₂ at 473 K (26). This step resulted in larger, but rather stable crystallites (33), specific surface 2.64 m² g⁻¹ (as determined by H₂–O₂ titration). Separate lots of the same batch of sample **2** were used for all measurements.

Electron Spectroscopy

Details of electron spectroscopy have been reported earlier (8, 15, 34). A Leybold LHS 12 MCD instrument was used (15, 19). UP spectra were measured with He I and He II excitation (21.2 and 40.8 eV, respectively, PE = 12 eV). Both Mg K α and Al K α anodes were used for XPS excitation, in the pass energy (PE) mode (PE = 48 eV). The binding energy (BE) was calibrated to the Au 4f_{7/2} line (BE = 84.0 eV). Difference spectra were obtained either by direct subtraction (35) or after normalizing the intensities at the BE value in the peak (36). The Pt 4f, O 1s, and C 1s peaks underwent satellite subtraction and Shirley background subtraction. Atomic compositions were determined from peak areas with literature sensitivity factors (37). The use of the homogeneous composition model in a powder-like sample with a very corrugated outer macroscopic surface seemed to be justified (34).

Electron Microscopy

A JEOL 2000FXII transmission electron microscope (TEM) was used to examine thin sections of various catalysts. The estimated point-to-point resolution of this instrument was 0.18 nm. Specimens were prepared by dispersing the catalyst powders in isobutyl alcohol and placing a drop of the suspension onto a holey carbon film. Using this approach, it was possible to locate sections of the catalyst grains that protruded over the edge of the carbon film without interference from the substrate. High-resolution electron micrographs were taken of several regions of a given specimen. Some micrographs underwent digital image processing.

Exposure to Hydrocarbon

The Pt black samples were purified by O₂-H₂ treatment and then exposed to *trans,trans*-2,4-hexadiene (24HD). Reactions performed in the preparation chamber of the photoelectron spectrometer were followed directly by electron spectroscopy (12, 15). Five exposures with 24HD were carried out: **2/1a**, 24HD alone, 13 mbar, 603 K, 20 min; **2/1b**, 24HD alone, 53 mbar, 603 K, 40 min; **2/2a**, 24HD alone, 53 mbar, 603 K, 20 min; **2/2b**, 53 mbar of 24HD + 13 mbar of H₂, 10 min at 693 K; **2/3**, 42 mbar of 24HD + 210 mbar of H₂, 603 K, 20 min, with regeneration in between. The overall composition of the as-received samples as well as the 24HD-treated and regenerated catalysts is shown in Table 1. Samples **1**, **2**, **2/1b**, **2/2b**, and **2/3** were taken out from the spectrometer and subsequently examined by TEM. This indicates that three samples, **2/1**, **2/2**, and **2/3**, were used, **a** and **b** indicating two subsequent runs with regeneration in between (cf. Table 1).

Another catalyst sample (50 mg) was subjected to analogous treatments in a closed-loop glass catalytic reactor system mimicking the exposures in the spectrometer as closely as possible (9, 12). Product analysis by gas chromatography was used to check upon the transformation of 24HD during its 20-min contact with Pt black. Test runs of 50 min under standard conditions followed exposures in the catalytic reactor: 10 Torr of *n*-hexane and 120 Torr of H₂, without regenerating the catalyst (12). By following this protocol, it was possible to monitor the residual activity and selectivity after 24HD treatments of differing severity. Four subsequent sampling steps during the test run gave information on the possible self-regeneration.

TABLE 1

Composition of Pt Black Samples after Various Treatments

Sample and treatment	Composition (at.%) ^a		
	Pt 4f	C 1s	O 1s
1 (→independent TEM)	67	24	9
2 as is (→independent TEM)	73	18	9
O ₂ , H ₂ regeneration before 2/1a	77	18	5
2/1a (HD, 13 mbar, 603 K, 20 min)	51	47	2
O ₂ , H ₂ regeneration after 2/1a	68	28	4
2/1b (HD, 53 mbar, 603 K, 40 min)	48	51	1
→ to TEM			
O ₂ , H ₂ regeneration before 2/2a	75	22	3
2/2a (HD, 53 mbar, 603 K, 20 min)	50	48	2
H ₂ after 2/2a	52	46	2
O ₂ , H ₂ regeneration after 2/2a	69	29	2
2/2b (HD, 53 mbar; H ₂ , 13 mbar, 693 K, 10 min) → to TEM	49	50	1
Regenerated before 2/3	72	26	2
2/3 (HD, 42 mbar; H ₂ , 210 mbar, 693 K, 20 min) → to TEM	55	44	1

^a Calculated from the area of the peaks shown, using literature sensitivity factors.

RESULTS

Catalyst Carbonization

Metal-catalyzed stepwise aromatization of the *n*-C₆ chain (38, 39) may involve diene intermediates. *cis*-Hexadienes should precede benzene formation, whereas *trans* isomers were coke precursors. As a consequence, 24HD could cause a more rapid carbonization than hexane.

24HD itself could also undergo catalytic transformations during its contact with Pt in the preparation chamber and in the glass reactor. A product analysis in the latter case permitted us to calculate TOF values of hexadiene transformation *during exposure*. No particular importance can be attributed to absolute TOF values; however, their comparative values may be informative. Treatment **2/1a** can be taken as a reference. Using a higher hydrocarbon pressure in **2/1b** gave a higher TOF than **2/1a**. (Sample **2/2a** was analogous to **2/1b**, reproduced well those values, and will not be discussed in detail.) Even a small amount of H₂ (and also the higher temperature with sample **2/2b**) gave rise to a significant increase in the transformed amount of 24HD. The slight increase of the overall pressure at the end of the exposures in the preparation chamber (corresponding roughly to the TOF values shown in Table 2) is in agreement with these results and was probably due to dehydrocyclization of 24HD to benzene, with H₂ being evolved:



The selectivities were rather similar during exposures **2/1a**, **2/1b**, and **2/2b**, with double-bond isomerization being the main process. The length of exposure had a minor influence on the chemical composition measured after its completion (cf. footnote to Table 2). The low amount of added H₂ did not result in a marked hydrogenation reaction in the case of **2/2b** as opposed to **2/3** with a large H₂ excess (**2/3**), where hydrogenation was the prevailing reaction (Table 2).

The overall activity *after deactivating treatments* was checked in standard test runs (20) with an *n*-hexane/hydrogen mixture (nH:H₂ = 13:160 mbar). The residual activity dropped to about 8–13% of the original value as compared to regenerated Pt (Table 3). Two distinct behavior patterns were observed during long runs of 50 min. Two samples, **2/1a** and **2/3**, exhibited a higher residual activity and also showed some self-reactivation. The residual activities after **2/1b** and **2/2b** were lower and remained virtually constant up to 35 min, when a very slight reactivation was observed (Table 3).

Isomers (methylpentanes), methylcyclopentane (MCP), alkane fragments, and benzene were produced in nearly equal amounts on a regenerated Pt. The formation of the first three product classes was suppressed selectively on deactivated samples (40, 41). This nonuniform deactivation

TABLE 2
Transformation of 24HD during Deactivating Runs

Treatment ^a	TOF (h ⁻¹)		Product distribution (%)				
	Initial ^b	Overall ^b	<C ₆	nH ^c	Hexenes	Dienes ^d	Benzene
2/1a (HD, 13 mbar, 603 K)	4	2	2	2	1.5	89.5	5
2/1b (HD, 53 mbar, 603 K, 40 min)	12	5	1	2	1	91	5
2/2a (HD, 53 mbar, 603 K)	13	7	2	4	2	87	5
2/2b (HD, 53 mbar; H ₂ , 13 mbar, 693 K) ^e	51	30	1	2	2	85	10
2/3 (HD, 42 mbar; H ₂ , 210 mbar, 693 K)	310	83	2.5	89 ^f	1.5	~0	2.5

^a Catalyst mass: 50 mg. Exposure to 24HD: 20 min, except for **2/1b**, where it lasted for 40 min. Typical conversions were ~30% for **2/2b** and nearly 100% for **2/3** as opposed to 5–6% for other treatments. The turnover frequencies given were related to the whole length of the run; the initial values (measured after 5 min) were about twice as high.

^b Initial: measured after 5-min contact time; overall: measured over the whole period of hydrocarbon exposure.

^c *n*-Hexane.

^d Geometric and double-bond isomerization, mainly to *cis*/*trans*-24HD and 1,3-hexadiene, with much less *cis,cis*-24HD and 1,4-hexadiene.

^e TOF after an exposure of 10 min (the equivalent of the treatment carried out in the spectrometer) was 35 h⁻¹ and the product distributions were almost the same (e.g., 2% hexenes, 88% dienes, 8% benzene).

^f Plus 4.5% 2- and 3-methylpentane and methylcyclopentane (MCP).

behavior was different from that observed on bifunctional catalysts (42). This phenomenon appeared in the present experiments after all pretreatments with 24HD, with a simultaneous slight increase of benzene and pronounced augmentation of hexene selectivity (Fig. 1). The selectivities also exhibited more marked changes after various pretreatments than residual activities. The former two groups also manifested themselves here: **2/1a** and **2/3** (with ~12% activity left) produced more C₆ saturated products and fragments than **2/1b** and **2/2b**, where dehydrogenation to hexene predominated together with some aromatization. The

most severe deactivation *and* selectivity shift were observed after pretreatment **2/1b**. In contrast, although treatment **2/3** resulted in a decline of the residual activity by a factor of 8, hardly any alteration was seen in the selectivity values (Table 3 and Fig. 2).

The selectivities of deactivated Pt samples during self-reactivation were related to the values found on the regenerated catalysts and these data are plotted in Fig. 2. The existence of two behavioral patterns was also apparent in these samples. The catalysts subjected to the less severe pretreatments **2/1a** and **2/3** exhibited a lower initial activity loss and noticeable reactivation demonstrated a diminishing relative hexene selectivity during reaction. The values

TABLE 3

Percent Residual Activity in Test Runs on Regenerated Pt and after Carbonizing Treatments^a

Sample ^b	Sampling time (min)				ΔC (%) ^c
	5	20	35	50	
TOF on regenerated Pt (h ⁻¹)	17.6	8.05	5.85	4.80	
Relative activity after different treatments ^d					
Regenerated Pt	100	100	100	100	
2/1a	12.1	14.8	16.5	17.4	19
2/1b	8.1	7.9	7.8	11.5	23
2/2a	8.0	7.3	7.8	9.3	20
2/2b	7.3	7.3	7.4	10.8	22
2/3	12.7	23.4	28.5	32.1	16

^a In test runs with *n*-hexane at 603 K, $p(\text{nH}) : p(\text{H}_2) = 10 : 120$ Torr. The percent relative activity was calculated from the value measured after identical sampling times.

^b After treatment with 24HD as shown in Tables 1 and 2.

^c The increment of carbon content (in percentage of the total surface) after various treatments from the reproducible level of residual carbon percentage in regenerated Pt (taken as 28%; cf. Table 1).

^d Related to the activity of regenerated Pt (TOF = 100).

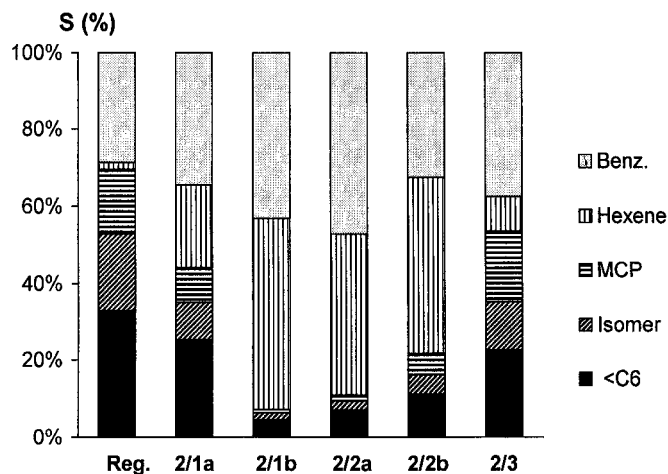


FIG. 1. Actual selectivities of *n*-hexane transformation in test runs ($\text{nH} : \text{H}_2 = 13 : 160$ mbar, 603 K) on a regenerated catalyst and on samples exposed to 24HD at different pressures as shown in Tables 1 and 2. Sampling time: 5 min.

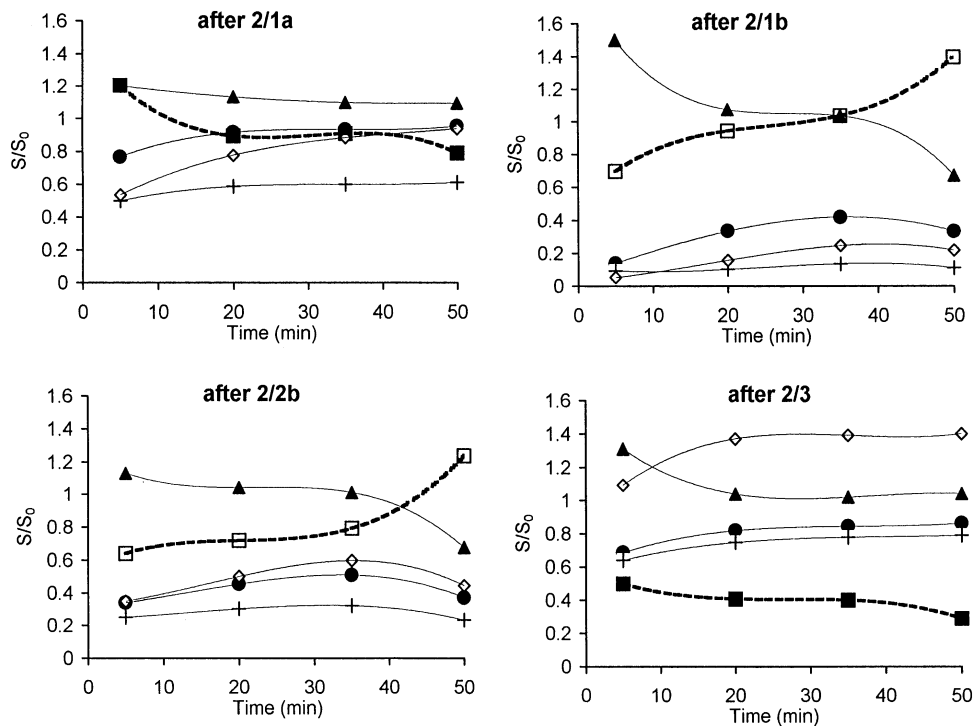


FIG. 2. Selectivities in test runs of 50 min with $nH_2 = 13:160$ mbar after different deactivating treatments, related to the selectivities measured on regenerated Pt, S/S_0 , where S_0 is the respective selectivity over regenerated Pt and S is the selectivity after deactivating treatments related to S_0 measured after the same length of run. Pretreatments **2/1a**, **2/1b**, **2/2b**, and **2/3**, respectively, are shown in the panels. Symbols: (●) hydrogenolysis; (+) skeletal isomers; (◇) methylcyclopentane; (▲) benzene. The relative selectivities of hexene increased and had to be scaled down to accommodate the curves in the same gradation: (■) hexenes/10; (□) hexenes/40.

for fragmentation and MCP grew simultaneously whereas the ability to isomerize was retarded (Fig. 2). The higher initial hexene selectivity observed with samples **2/1b** and **2/2b** (Fig. 2) increased further during the run and showed an appreciable drop in benzene selectivities. The other low values did not show considerable variations. Note the enhanced initial aromatic selectivities in both cases and their progressive decrease during reaction. Benzene selectivity always decreased. The two cyclic products—benzene and MCP—showed an interesting “mirror image” after pretreatment **2/3**, the values of MCP during the test run exceeding those measured on regenerated Pt, but similar behavior was seen in all cases in Fig. 2. This may point to nonuniform reactivation of all sites: hydrogen can remove benzene precursors but those sites can produce MCP only. In this state, surface hydrogen would control the fate of the primary chemisorbed intermediate: toward a deeply dehydrogenated one for benzene or to a less dehydrogenated one for C_5 cyclization (43).

Valence States of Surface Components

As can be seen from Table 1, while all catalyst samples contained carbon and oxygen impurities, a presintering treatment increased the purity (cf. samples **1** and **2**).

An initial regeneration of Pt stored in air did not improve the purity markedly except decreasing the O 1s contribution, first of all, in the PtO region. The oxygen region contained mainly adsorbed OH (BE ~ 531.5 eV) when transferred into the vacuum chamber. The residual O after various treatments contained mostly adsorbed water (BE ~ 532.5 eV) and some oxidized C (BE > 533 eV) (8, 12, 34). The adsorbed O component was negligible, as opposed to Pt reduced by hydrazine (8). This finding agrees well with the Pt 4f spectra shown in Fig. 3, indicating mainly pure Pt^0 (BE maximum of Pt 4f_{7/2} around 71.1 eV). A very small minimum in the difference spectrum **2** – **1** indicates a minor enhancement of the metallic state upon sintering. The difference between the carbon-covered Pt (**2/1b**) and Pt regenerated before **2/1** was even less, in spite of a much lower platinum percentage in the former case. This finding suggests that there is very little electronic interaction between Pt and its major impurity, C (44).

The unsintered and presintered Pt (samples **1** and **2**) also contained some oxidized carbon at BE > 286 eV (8). Mostly graphitic C seemed to be present after O_2 – H_2 treatments (Fig. 4). A marked carbon accumulation was observed upon exposure to 24HD, the percentage of which increased up to 44–51%. Samples exposed to 24HD showed nearly identical C 1s peaks (Fig. 4). Hydrogen treatment alone (carried

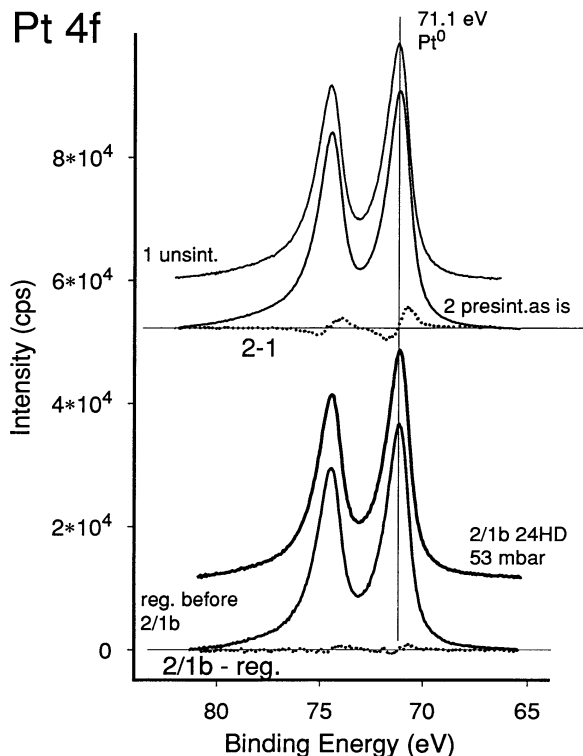


FIG. 3. Pt 4f region of the unsintered and presintered catalysts as well as after 24HD exposure and in the regenerated state, together with two respective difference spectra, calculated after intensity normalization.

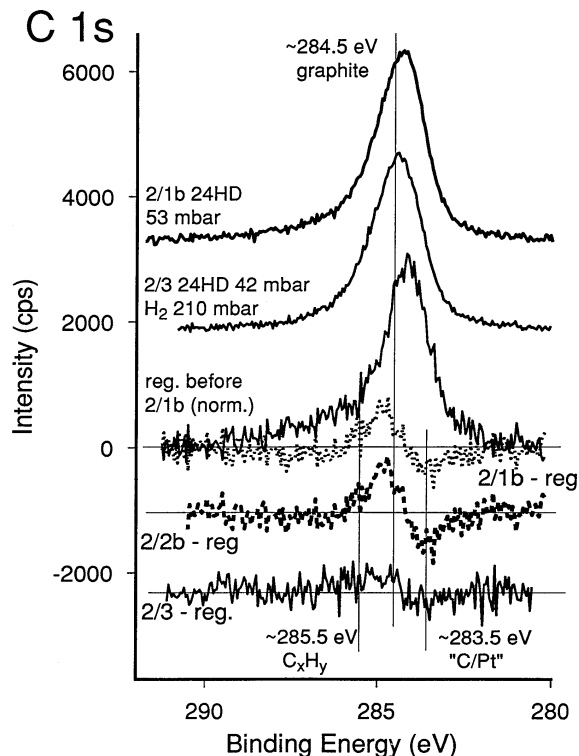


FIG. 5. C 1s spectra of a regenerated catalyst (normalized to **2/1b**) and after two different HD exposures: 24HD alone (**2/1b**) and 24HD with excess H₂ (**2/3**).

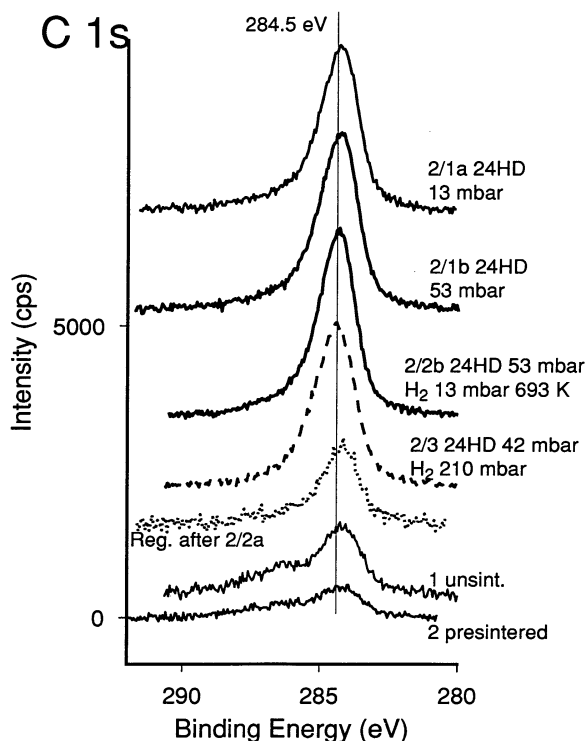


FIG. 4. C 1s region of the unsintered and presintered catalysts as well as after four 24HD exposures, together with a C 1s peak of a typical regenerated catalyst. The spectra show the original measured intensities.

out after **2/2a**) removed minor amounts of carbon, both graphite and C_xH_y. Full regenerations with O₂/H₂ removed less than half of the surface carbon (C: 28–29%) but the residual carbon was still more than after the first regeneration (C ~ 18% before **2/1**). The normalized C 1s spectra of regenerated catalysts *before* and *after* 24HD treatments were again almost identical (12). The BE maximum of regenerated samples was lower than that corresponding to pure graphitic carbon. This points to the presence of C/Pt entities at BE ~ 283.5 eV. C/Pt denotes here surface or intercalated C atoms rather than carbidic species (35). This is well illustrated by the difference spectra in Fig. 5 (**2/1b - reg.**, **2/2b - reg.**, **2/3 - reg.**). They all show an excess of graphite in the carbonized catalysts (positive peak) and the appearance of excess Pt/C after regeneration (negative peak). All difference spectra are analogous, although the peak sizes are different: they increase parallel to the severity of treatments. The difference spectra between carbonized and regenerated samples are all similar, which was checked by using two regenerated spectra, too.

C 1s difference spectra between various exposures may be more informative (Fig. 6). Samples **2/1a** and **2/3** (with highest residual activity and lowest increase of carbon content; Table 3) were taken as references. The top spectrum indicates that a higher pressure of 24HD (sample **2/1b** vs **2/1a**) slightly increased the graphitic component. A more

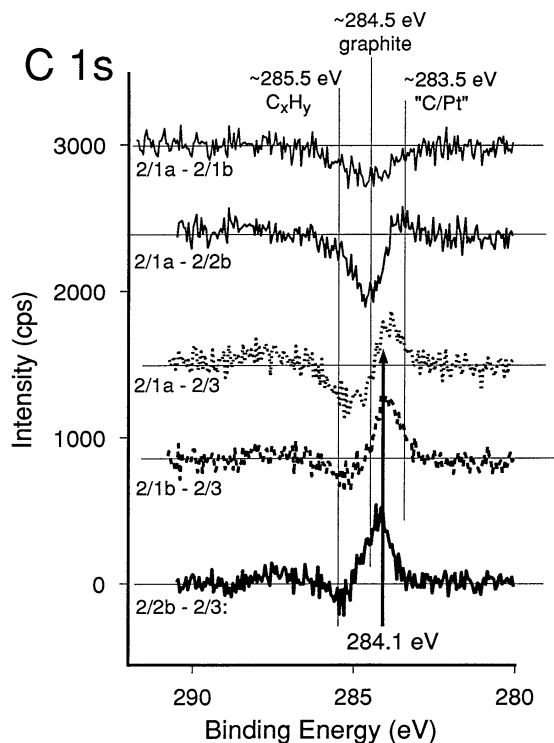


FIG. 6. C 1s difference spectra of samples subjected to various exposures. Subtraction was carried out without intensity normalization.

pronounced increase took place after treatment **2/2b** (at higher temperature). A small excess of a component with BE ~ 284.1 eV appeared in **2/2b**. This C 1s component prevailed when the spectrum of **2/3** was subtracted from that of other samples. The lower three difference spectra in Fig. 6 show higher and higher intensities for it as the severity of treatment compared to **2/3** increased (**2/1a** < **2/1b** < **2/2b**). **2/3** contained more graphitic C than **2/1a** (as shown by a dip in the difference spectrum), although their residual activity and selectivity patterns in the *n*-hexane test run were rather similar (Fig. 2 and Table 3). The amount of graphite in samples **2/1b** and **2/2b** gradually reached that of **2/3**. The component at ~ 284.1 eV may be some intermediate carbon species of individual C atoms in the act of polymerization to graphite-like entities (35).

Fitting individual components to the C 1s peak (8, 34) confirms the higher—and almost equal—abundance of the deactivating component (BE = 284.1 eV) in **2/1a**, **2/1b**, and **2/2b**. More graphitic C (and also C_xH_y) was present in sample **2/3** (Table 4). The contribution of oxidized C was minor and the wider range of maximum BE values indicates different main components (with C–O or C=O bonds). Regeneration removed about half of both the deactivating and graphitic components.

The carbon accumulation following various exposures is well demonstrated by UPS. A regenerated Pt catalyst showed rather high Fermi-edge intensity in He I (Fig. 7).

TABLE 4

Percent Distribution of C 1s Components on Selected Carbonized and Regenerated Samples^a

Sample	C 1s component ^b				
	Pt/C	Disordered C	Graphitic	C_xH_y	Oxidized C
2/1a	2	28	11	5	1
Regenerated after 2/1a	3	14	6	3	2
2/1b	2	26	14	6	3
2/2b	2	25	14	6	3
2/3	2	12	18	9	3

^a After treatment with 24HD as shown in Tables 1 and 2, in percentage of the *total* surface. The carbon content of individual samples is shown in Table 1. The fitting used mixed Gaussian–Lorentzian curves with a fwhm of 1.3 eV (or 1.4 and 1.7 eV for the two highest BE peaks). The fitting was carried out in a self-consistent manner; i.e., the peak maxima had to be found by the fitting process itself.

^b The BE values found by the self-consistent fitting program for the individual components are as follows: Pt/C, 282.6–282.8 eV; disordered carbon species, 284.0–284.1 eV; graphitic carbon, 284.7–284.8 eV; C_xH_y polymers, 285.6–286 eV; oxidized carbon species, 286.8–287.8 eV.

Carbon accumulation suppressed largely the Fermi-edge intensity (45); the “buckle” at medium BE values (~ 5 –8 eV) evidenced the presence of overlayer-type carbon rather than chemisorbed hydrocarbon molecules (8, 34, 46). The He II difference spectrum **2/3** – **reg** (Fig. 8) confirmed the accumulation of a massive carbon layer after **2/3** producing the lowest carbon content (Table 1). This was, however, graphitic (Fig. 6).

Electron Microscopic Examination

The particles of the fresh catalysts (sample **1**) were hexagonal in shape and relatively thin, as shown by the lattice fringes. A survey of many specimen fields suggested that the metal particle widths ranged from 5 to 15 nm. The quite

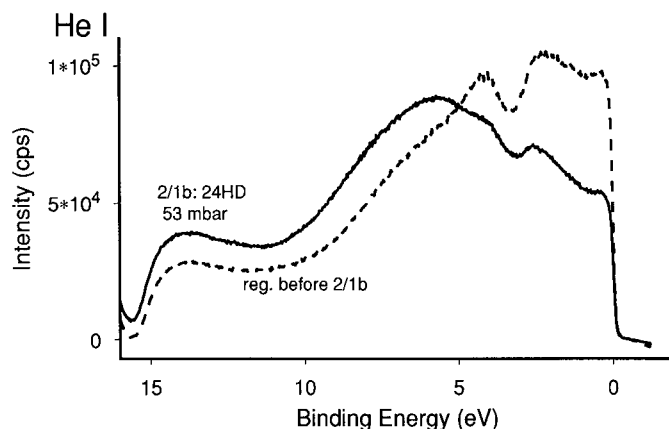


FIG. 7. He I UP spectra of a regenerated catalyst and after exposure to 53 mbar of 24HD (**2/1b**).

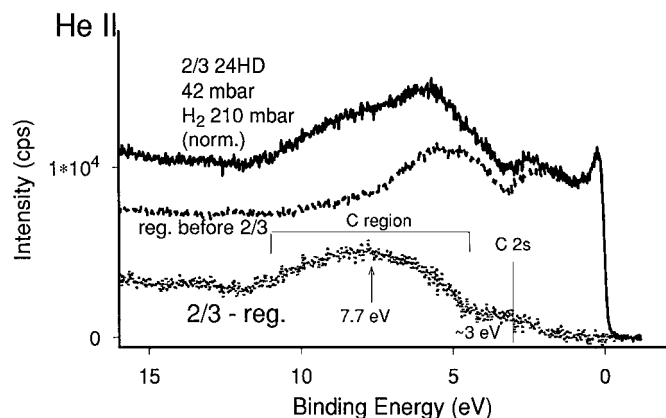


FIG. 8. He II UP spectra of a regenerated catalyst and after exposure to 24HD with excess H_2 (**2/3**). The difference spectrum was calculated after normalizing the intensity of **2/3** at the Fermi edge (BE = 0).

uniform density across the structure indicated a pillbox geometry. TEM gave evidence for the presence of some amorphous carbon around the edges of highly faceted platinum crystallites (Fig. 9).

TEM confirmed the major particle size growth after presintering of sample **1** to sample **2** (8, 26, 33). A relative large crystallite is seen in Fig. 10, with lattice fringes of 0.22 nm (47) corresponding to Pt(111). Inspection of the catalyst surface shows the existence of an overlayer of pyrolytic carbon consisting of curved layer fragments along the particle. Since the presence of this type of carbon was

far from being uniform, it cannot be attributed to *in situ* carbon formation in the microscope chamber. The pillbox geometry of this grain has apparently remained and this aspect did not change upon exposure to 24HD. Figure 11 shows two Pt crystallites after exposure **2/1b**. Figure 11A shows the Pt(111) lattice fringes covered by the pyrolytic carbon overlayer. Another section of the same micrograph (Fig. 11B) depicts a reconstructed Pt surface, the (111) lattice fringes showing a spectacular turn in the outermost layer of ~ 1 nm (area a). The carbonaceous deposit after treatment **2/2b** (at higher temperature but in the presence of H_2) contained graphite-like layers growing outward from the Pt surface, i.e., their edges being in contact with Pt (Fig. 12A, area C; see also Fig. 12B). This aspect was confirmed by its lattice spacing corresponding to the well-established value for the spacing between consecutive graphite layers: 0.335 nm (17). This graphitic carbon was, however, far from an ordered structure. A similar but thicker graphite-like overlayer appeared after treatment **2/3** (Fig. 13, area A). It coexisted with the overlayer-type carbon (area B). This finding may be in agreement with the statement that the presence of hydrogen promoted the graphitization of initially formed surface polymers (16).

One has to remember that the rather marked Pt percentages (Table 1) indicate that the thickness of *any* carbonaceous overlayer is not uniform over all particles (8): the micrographs reveal the structure of massive three-dimensional deposits in numerous places where their dimensions were sufficient for microscopic observation.

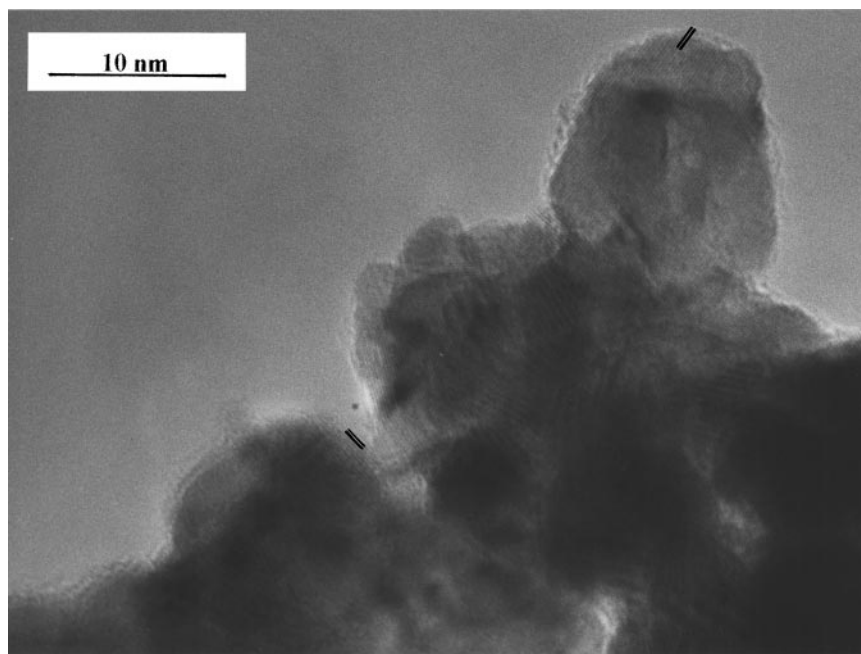


FIG. 9. Electron micrograph of unsintered Pt (sample **1**). Note the Pt lattice fringes (as shown) and the carbonaceous overlayer around the top-right crystallite.

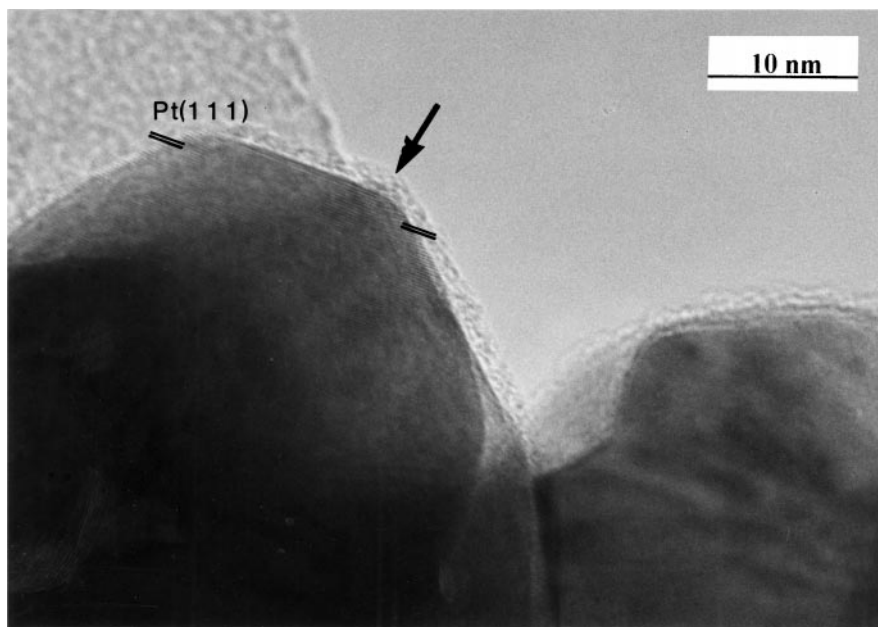


FIG. 10. Electron micrograph of sintered, untreated Pt (sample 2). The crystallite growth is obvious but the Pt(111) lattice fringes and the presence of carbonaceous overlayer (arrow) are clearly seen.

DISCUSSION

It is not surprising that exposure to hydrocarbons leads to accumulation of carbonaceous entities on Pt and that these species lead to catalyst deactivation (4, 14, 18, 48, 49). We believe, however, that the present results add new information on the amount and likely chemical state of surface carbon, and the data reveal new correlations between surface carbon and the catalytic properties of platinum.

Of the enormous variety of possible carbon structures (17), Fig. 14 summarizes some entities that can exist on Pt surfaces, together with the corresponding C 1s BE values. Final and irreversible catalyst deactivation is usually attributed to graphite but there are several (sometimes poorly defined) intermediates preceding this stage (50). As mentioned above, single C atoms are sometimes regarded as the first step of catalyst carbonization (14, 50). Regeneration by O₂ and H₂ also involved structural rearrangement

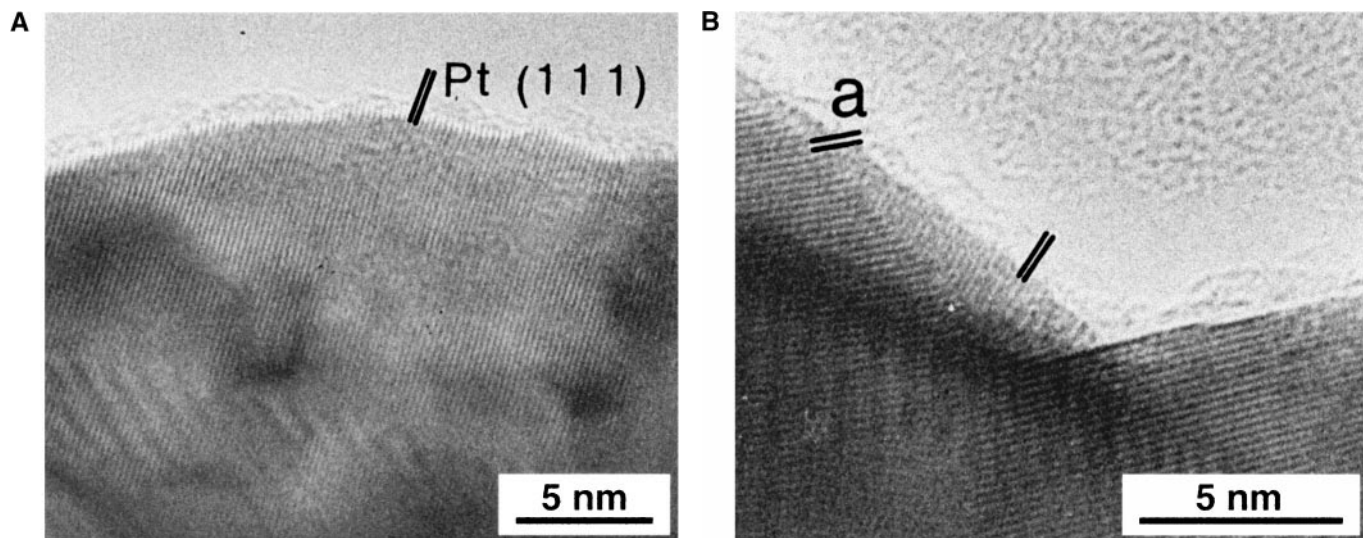


FIG. 11. Two digitally processed areas of the same micrograph of sample 2/1b after treatment of Pt with 13 mbar of 24HD at 603 K. The Pt(111) lattice fringes are clearly seen in A, together with the rather amorphous carbonaceous overlayer. A surface recrystallization is seen in B: the fringes in area a point to a direction different from the unmarked area in the middle of the picture.

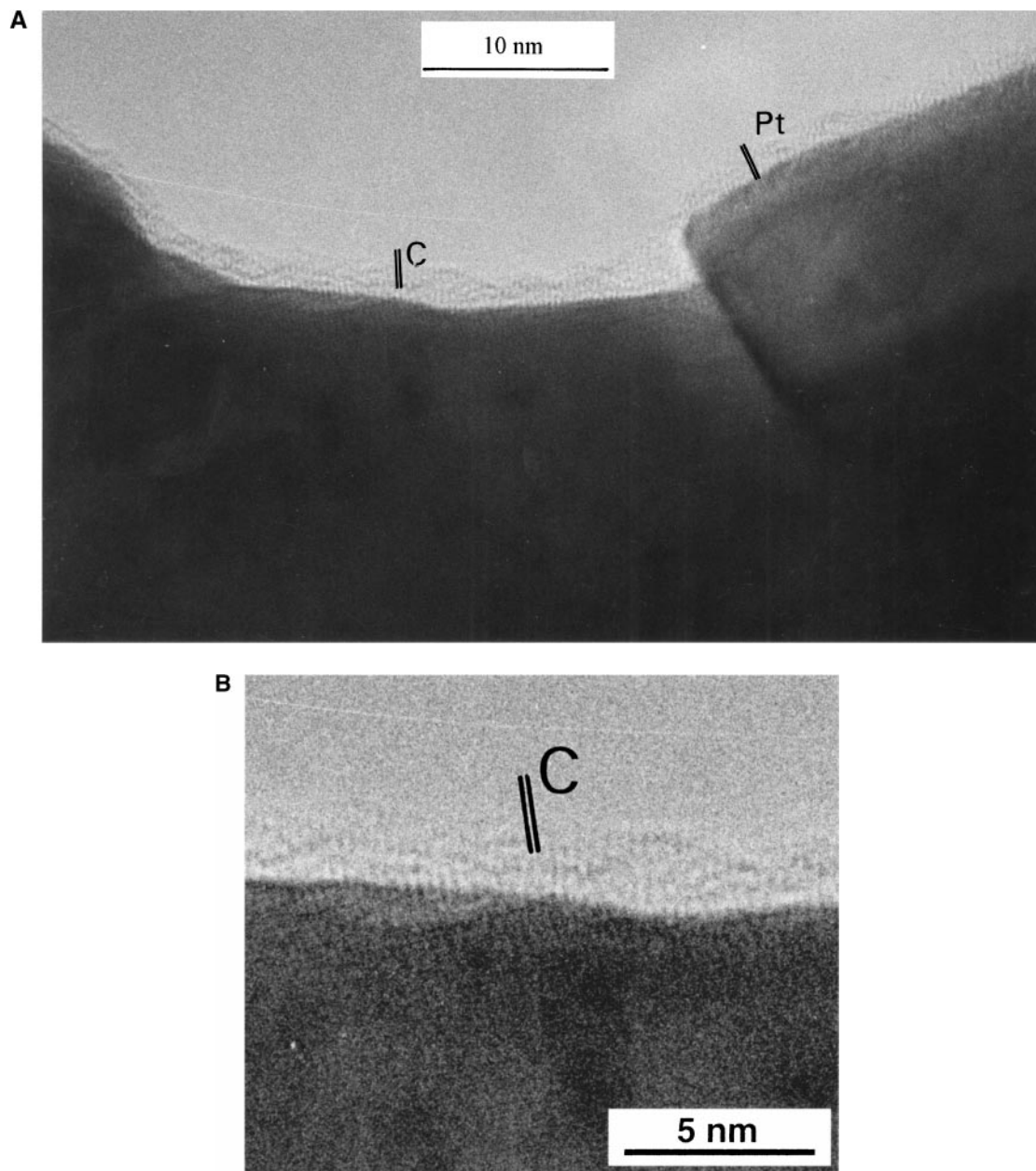


FIG. 12. Electron microscopy of sample **2/2b** treated with 24HD in the presence of a low amount of added H_2 . Pt(111) lattice fringes are present. The digitized image B shows lattice fringes of rather disordered graphite layers in area C, contacting through their *edges* with the Pt surface. Layer distance, ~ 0.34 nm (17).

of Pt (15), accompanied by the migration of C atoms between surface and subsurface positions. The disruption of contiguous carbon layers may lead to the enhancement of Pt-C entities (Fig. 5).

Table 1 shows that although a higher temperature, a higher hydrocarbon, and lower hydrogen pressure resulted in the formation of somewhat more solid carbon, the differences in the final C percentages were rather small. Table 3 confirms that the increase of the percent carbon and the overall activity decrease were not strictly proportional. The

difference spectra in Fig. 5 offer a semiquantitative estimation of the increase of surface graphite (as compared with the regenerated state). We suggest, therefore, that the main reason for the attenuation of overall activity (Table 3) was the covering of active sites by contiguous carbonaceous deposits, of which graphite must be a major component after each exposure. At the same time, the residual activity after the least severe treatments (**2/1a** and especially with sample **2/3** treated in excess H_2) was higher than that found with the other samples and the selectivity pattern was

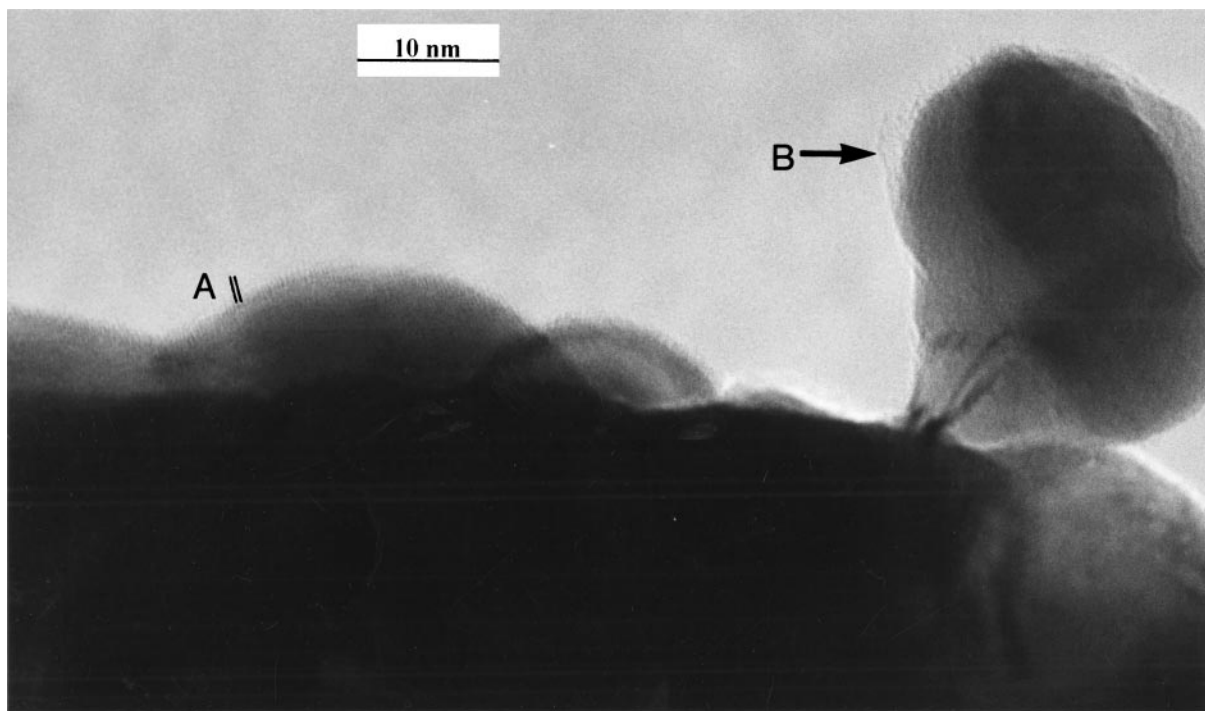


FIG. 13. Electron microscopy of sample **2/3** treated with 24HD in the presence of a high amount of added H_2 . Hardly any Pt lattice fringes are seen. The fringes in area A correspond to that of graphite, the layers pointing outward from the Pt surface, as in Fig. 12. They coexist with amorphous carbonaceous overlayers (area B).

closer to that of the regenerated catalyst (Table 3). Thus, a component different from graphitic carbon must have been responsible for (i) the dramatic selectivity changes resulting in hexenes as the main products and (ii) the lack of spontaneous reactivation in the *n*-hexane/ H_2 test runs. Indeed, another C 1s component at BE ~ 284.1 eV appeared in the difference spectra between those samples and **2/3** (Fig. 6). Its exact spectroscopic identification is not easy. Freyer *et al.* (35) attributed a shift of the C 1s maximum from ~ 283.5 to ~ 284.5 eV to a gradual transformation of single C atoms from chemisorbed ethylene to graphitic entities, ethylidyne predominating at the intermediate binding energies. However, their adsorbent, ethene, is a much simpler molecule. The differences between surface carbon produced on Pt even from ethene and propene were rather pronounced (51). In fact, molecular structures could be depicted for the fate of a C_2 adsorbate as opposed to the rather schematic picture for higher hydrocarbons (49). 24HD, with six C atoms in its chain, offers a large variety of chemisorption. We believe therefore that C_6 molecules or various (larger) fragments as well as their oligomers, likely attached by one or more multiple Pt–C bonds to the metal surface (52), may correspond to the disordered carbon at BE ~ 284.1 eV. This species, called “chain hydrocarbons” in Fig. 14, may include several surface entities, representing precursors of graphitic or aliphatic polymers. Török *et al.* (53) attributed deactivation of Pt mainly

to a disordered carbon moiety, which they identified also by IR spectroscopy. Our results indicate that these entities inhibit first of all skeletal reactions, requiring multiple ensembles (54). Hence, the selectivities of isomers and C_5 cyclic products decreased. However, since these entities likely have low molecular weight (e.g., C_{12} – C_{24}), we cannot expect their appearance in electron microscopy. They may have the partly chainlike, partly macrocyclic, unsaturated nongraphitic structure observed by McCarroll *et al.* (55) and may be intermediates of coke formation (50).

The carbon remaining on regenerated Pt black catalyst may be similar to the “residual” carbon suggested by Garin *et al.* (7). The amount of this material (18–28%; Table 1) is, however, much higher in our case than the carbon percentage they found (4%) on Pt single-crystal surfaces. Since catalyst activity is restored reproducibly, carbon in this state must correspond—from the catalytic point of view—to the “harmless” or “invisible” type of deposit (56). The percentage of solid carbon increased to ~ 44 –50% upon various exposures to 24HD. The higher amount of residual carbon on our dispersed unsupported catalyst with a more flexible surface (57) may be related to the mobility of carbon between subsurface and surface positions. At the same time, we present new experimental evidence supporting the accumulation of three-dimensional carbon proposed earlier on single-crystal (2, 3) as well as dispersed Pt surfaces (8). Faceting occurred even on a Pt foil at ca. 600 K (58) but

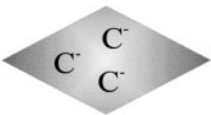

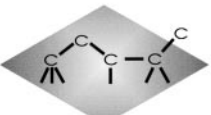


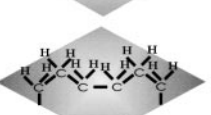

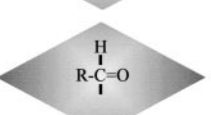
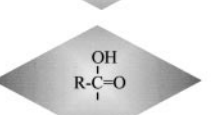
Carbide		282.5 eV
Isolated carbon		283.8 eV
"Chain" carbon		284.1 eV
Graphene		284.4 eV
Graphitic carbon		284.6 eV
Aliphatic polymers		285.0 eV
Alcohol groups		286.0 eV
Keto groups		287.0 eV
Carboxylic groups		288.5 eV

FIG. 14. Schematic representation of carbon species that are possible on platinum surfaces and their respective C 1s binding energies. BE values were taken from the literature (8, 17, 36, 46) as well as from unpublished results from the Department of Inorganic Chemistry, Fritz-Haber-Institut.

carbon deposition—a mixture of graphite and disordered C—was reported (10) at higher temperatures than those used in the current investigation (>850 K).

This is the first experimental report in which transmission electron microscopy has been used to demonstrate the presence of three-dimensional graphitic carbon on the Pt surface. The location of graphitic overlayers was almost perpendicular to the outer surface of Pt, corresponding to the initial, rudimentary steps of ribbon-like graphite growth (59). The minor amounts of oxygenated carbon species (Table 4)—as one of the structures shown in Fig. 14—may be present at the outer edges of the graphite layers. They can be detected in sample **2/2b** as a slight maximum at ~286–

287 eV in the difference spectrum **2/2b** – **2/3** (Fig. 6). Different values were reported for the C 1s BE of graphite (35, 46, 60). We found the BE of a highly ordered pyrolytic graphite, 284.6 eV, thus attributing 284.1 eV to a much less ordered structure can be realistic in our case. The line broadening and shift of BE to lower values upon destructive treatments (such as Ar⁺ ion sputtering) of graphite (46) can be attributed to the appearance of these partly decomposed lower BE components. The same behavior was observed with other ordered carbon structures, such as C₃N₄ (61).

The presence of hydrogen during pretreatment with 24HD proved to be decisive in determining the subsequent state and activity of the Pt catalyst. Even the minor reactions that occurred during the deactivating exposure by 24HD (double-bond shift and *trans*–*cis* isomerization of C=C bonds; Table 2) required hydrogen (62). These reactions could utilize hydrogen “retained” by Pt (40, 63) or H given off during benzene formation (Table 2). Excess H₂ during exposure (sample **2/3**) was found to accelerate the catalytic reactions of 24HD and, as a consequence, also promoted solid carbon accumulation. This finding agrees well with the report by McAllister and Wolf (22), who found that more hydrogen preserved the catalytic activity not only in the traditional sense (i.e., in forming useful products; cf. Table 2) but also that of the deactivation reaction, i.e., the process between the gas and the solid surface resulting in high molecular weight residues was more rapid in H₂. This polymer would tend to be graphitized more easily; thus the mass of carbon accumulated in the presence of hydrogen could be relatively large (22). Dissolution of C in Pt, a well-known precursor of graphite nanofiber formation, was found to be promoted by the presence of hydrogen (16). Wetting of graphite by Pt is known to occur in the presence of hydrogen (16). The XRD pattern of Pt blacks showed a broad band corresponding to disordered surface graphite after treatment in hydrogen (13). Although one can never be sure that a feature *not* seen in TEM does not exist, one should remember that both micrographs where graphite layers—perpendicular to the surface—were identified (Figs. 11 and 12) originate from samples pretreated *in the presence of hydrogen*.

ACKNOWLEDGMENTS

The authors thank Mike Frongillo (Center for Materials Science and Engineering Electron Microscopy Facility, Massachusetts Institute of Technology) for his contributions in carrying out electron microscopy. We thank Prof. R. T. K. Baker for encouragement and helpful discussions. Z.P. thanks the DAAD for supporting his stay in Berlin, where electron spectroscopy was carried out. Additional financial support by an agreement between the National Science Foundation and the Hungarian Academy of Sciences is gratefully acknowledged. The catalytic measurements in Budapest were supported in part by the Hungarian National Scientific Research Fund (Grant OTKA T25599). The authors thank G. Glazer and É.

Hajmásy as well as the Group for Image Processing, Fritz-Haber-Institut, for their contribution in producing the final form of the electron micrographs.

REFERENCES

- Somorjai, G. A., and Zaera, F., *J. Phys. Chem.* **86**, 3070 (1982).
- Davis, S. M., Zaera, F., and Somorjai, G. A., *J. Catal.* **85**, 206 (1984).
- Zaera, F., Godbey, D., and Somorjai, G. A., *J. Catal.* **101**, 73 (1986).
- Webb, G., *Catal. Today* **7**, 139 (1990).
- Sárkány, A., *Catal. Today* **5**, 173 (1989).
- Sárkány, A., *J. Chem. Soc., Faraday Trans. 1* **85**, 1523 (1989).
- Garin, F., Maire, G., Zyade, S., Zauwen, M., Frennet, A., and Zielinski, P., *J. Mol. Catal.* **58**, 185 (1990).
- Paál, Z., Schlögl, R., and Ertl, G., *J. Chem. Soc., Faraday Trans.* **88**, 1179 (1992).
- Paál, Z., Xu, X. L., Paál-Lukács, J., Vogel, W., Muhler, M., and Schlögl, R., *J. Catal.* **152**, 252 (1995).
- Wu, N. L., and Phillips, J., *J. Catal.* **113**, 383 (1988).
- Van Langeveld, A. D., van Delft, F. C. M. J. M., and Ponc, V., *Surf. Sci.* **135**, 93 (1985).
- Paál, Z., Matusek, K., Wootsch, A., Wild, U., and Schlögl, R., Paper presented at the 16th North American Catalysis Society Meeting, Boston, 1999; *Catal. Today* **64**, 1 (2000).
- Find, J., Paál, Z., Sauer, H., Schlögl, R., Wild, U., and Wootsch, A., in "Proceedings, 12th International Congress on Catalysis, Granada, 2000" (*Stud. Surf. Sci. Catal.* **130**), p. 2291. Elsevier, Amsterdam, 2000.
- Sárkány, A., Lieske, H., Szilágyi, T., and Tóth, L., in "Proceedings, 8th International Congress on Catalysis, Berlin, 1984," Vol. 2, p. 613. Dechema, Frankfurt-am-Main, 1984.
- Find, J., Paál, Z., Schlögl, R., and Wild, U., *Catal. Lett.* **65**, 19 (2000).
- Owens, W. T., Rodriguez, N. M., and Baker, R. T. K., *J. Phys. Chem.* **96**, 5048 (1992).
- Schlögl, R., in "Handbook of Heterogeneous Catalysis" (G. Ertl, H. Knözinger, and J. Weitkamp, Eds.), Vol. 1, p. 138. Verlag Chemie, Weinheim, 1997.
- Ponc, V., *Adv. Catal.* **32**, 149 (1983).
- Paál, Z., Matusek, K., and Muhler, M., *Appl. Catal. A* **149**, 113 (1997).
- Paál, Z., Groeneweg, H., and Zimmer, H., *J. Chem. Soc., Faraday Trans.* **86**, 3159 (1990).
- Paál, Z., in "Hydrogen Effect in Catalysis" (Z. Paál and P. G. Menon, Eds.), p. 449. Dekker, New York, 1988.
- McAllister, P., and Wolf, E. E., *J. Catal.* **138**, 129 (1992).
- Somorjai, G. A., *J. Mol. Catal. A* **107**, 39 (1996).
- Nishiyama, S., Matsuura, S., Morita, H., Tsuruya, S., and Masai, M., *Appl. Catal.* **15**, 185 (1985).
- Schmidt, L. D., and Krause, K. R., *Catal. Today* **12**, 269 (1992).
- Baird, T., Paál, Z., and Thomson, S. J., *J. Chem. Soc., Faraday Trans. 1* **69**, 1237 (1973).
- Hlavathy, Z., and Tétényi, P., *Surf. Sci.* **410**, 39 (1998).
- Paál, Z., and Marton, D., *Appl. Surf. Sci.* **26**, 161 (1986).
- Fryer, J. R., and Paál, Z., *Carbon* **11**, 665 (1973).
- Davis, S. C., and Klabunde, K. J., *Chem. Rev.* **82**, 153 (1982).
- Chang, T. S., Rodriguez, N. M., and Baker, R. T. K., *J. Catal.* **123**, 486 (1990).
- O'Rear, D. J., Löffler, D. G., and Boudart, M., *J. Catal.* **94**, 225 (1985).
- Paál, Z., Zimmer, H., Günter, J. R., Schlögl, R., and Muhler, M., *J. Catal.* **119**, 146 (1989).
- Paál, Z., and Schlögl, R., *Surf. Interface Anal.* **19**, 524 (1992).
- Freyer, N., Pirug, G., and Bonzel, H. P., *Surf. Sci.* **126**, 487 (1983).
- Wild, U., Pfänder, R., and Schlögl, R., *Fresenius' J. Anal. Chem.* **357**, 420 (1997).
- Briggs, D., and Seah, M. P. (Eds.), in "Practical Surface Analysis," Vol. 1, Appendix 6, p. 635. Wiley, Chichester, 1990.
- Paál, Z., and Tétényi, P., *J. Catal.* **30**, 350 (1973).
- Paál, Z., *Adv. Catal.* **29**, 273 (1980).
- Paál, Z., Dobrovolszky, M., and Tétényi, P., *J. Catal.* **46**, 65 (1977).
- Paál, Z., Groeneweg, H., and Paál-Lukács, J., *J. Chem. Soc., Faraday Trans.* **86**, 3159 (1990).
- Marécot, P., and Barbier, J., in "Catalytic Naphtha Reforming" (G. J. Antos, A. M. Aitani, and J. M. Parera, Eds.), p. 279. Dekker, New York, 1995.
- Paál, Z., Székely, G., and Tétényi, P., *J. Catal.* **58**, 108 (1979).
- Sundararajan, R., Pető, G., Koltay, E., and Gucci, L., *Appl. Surf. Sci.* **90**, 165 (1995).
- Hugenschmidt, M. B., Dolle, P., Jupille, J., and Cassuto, A., *J. Vac. Sci. Technol. A* **7**, 3312 (1989).
- Schlögl, R., *Surf. Sci.* **189/190**, 861 (1987).
- JPCDS File 04-0802.
- Parera, J. M., and Figoli, N. S., in "Catalysis Specialists Periodical Reports" (J. J. Spivey, Ed.), Vol. 9, p. 65. Royal Soc. Chem., London, 1992.
- Bond, G. C., *Appl. Catal. A* **149**, 3 (1997).
- Biswas, J., Gray, P. G., and Do, D. D., *Appl. Catal.* **32**, 249 (1987) and references therein.
- Jackson, S. D., Hussain, N., and Munro, S., *J. Chem. Soc., Faraday Trans.* **94**, 955 (1998).
- Davis, S. M., Zaera, F., and Somorjai, G. A., *J. Catal.* **77**, 439 (1982).
- (a) Török, B., Molnár, Á., Pálkó, I., and Bartók, M., *J. Catal.* **145**, 295 (1994); (b) Fási, A., Kiss, J. T., Török, B., and Pálkó, I., *Appl. Catal. A* **200**, 189 (2000).
- Vogelzang, M. W., Botman, M. J. P., and Ponc, V., *Faraday Discuss. Chem. Soc.* **72**, 33 (1981).
- McCarroll, J. J., Edmonds, T., and Pitkethly, R. C., unpublished, cited by Moyes, R. B., and Wells, P. B., *Adv. Catal.* **23**, 121 (1973); Clarke, J. K. A., *Chem. Rev.* **75**, 297 (1975).
- Menon, P. G., *J. Mol. Catal.* **59**, 207 (1990).
- Somorjai, G. A., *J. Mol. Catal. A* **107**, 39 (1996).
- Wu, N. L., and Phillips, J., *J. Phys. Chem.* **89**, 591 (1985).
- Park, C., and Baker, R. T. K., *J. Phys. Chem. B* **102**, 5168 (1998).
- Belton, D. N., and Schmieg, S. J., *J. Vac. Sci. Technol. A* **8**, 2353 (1990).
- Bertóti, I., Tóth, A., Mohai, M., and Ujvári, T., *Surf. Interface Anal.* **30**, 538 (2000).
- Bond, G. C., in "Heterogeneous Catalysis," p. 138. Clarendon, Oxford, 1987.
- Paál, Z., and Thomson, S. J., *J. Catal.* **30**, 96 (1973).